Placental Insulin-like Growth Factor 1 Deficiency Drives Autism-Relevant Behavioral Changes with Sex-Specific Vulnerabilities

Annemarie J. Carver[1,2,3], Faith M. Fairbairn[2,3], Robert J. Taylor Jr.[2,3], Benjamin W.Q. Hing[2,3,4], Amrita Gajmer[2,3], Regan T. Fair[3,5,6], and Hanna E. Stevens[1,2,3,5,7]

[1]Interdisciplinary Graduate Program in Genetics, University of Iowa, IA, USA
[2]Department of Psychiatry, Carver College of Medicine, University of Iowa, IA, USA
[3]Iowa Neuroscience Institute, Carver College of Medicine, University of Iowa, IA, USA
[4]Department of Molecular Physiology and Biophysics, Carver College of Medicine, University of Iowa, IA, USA
[5]Interdisciplinary Graduate Program in Neuroscience, University of Iowa, IA, USA
[6]Department of Neuroscience and Pharmacology, Carver College of Medicine, University of Iowa
[7]Hawk-Intellectual and Developmental Disabilities Research Center, University of Iowa, IA, USA

Corresponding authors: Annemarie J. Carver (annemarie-carver@uiowa.edu) and Hanna E. Stevens (hanna-stevens@uiowa.edu)

Running title: Placental *Igf1* Insufficiency Influences Autism-Risk

Keywords: Placenta, Neurodevelopment, Insulin-like Growth Factor 1, Neuroplacentology, Preterm Birth, Autism Spectrum Disorder

Abstract:

Background:

Preterm birth and other perinatal adversities lead to the loss of placental support including critical hormones, such as insulin-like growth factor 1 (IGF1), required for neurodevelopment. Decreased IGF1 and preterm birth are associated with neurodevelopmental disorder risk, including autism spectrum disorder. Whether placental *Igf1* insufficiency drives neurodevelopmental risks is not understood.

Methods:

To understand these mechanisms, placental-targeted CRISPR manipulation in mice was employed to create placental *Igf1* insufficiency. Subsequently, embryonic forebrain development was assessed sex-specifically to identify structural and transcriptomic changes. Postnatal offspring were used to determine neurobehavioral trajectories relevant to neurodevelopmental disorders as assessed through learning, motor, and affective behavioral tasks and neurostereology.

Results:

Placental *Igf1* insufficiency reduced embryonic forebrain growth, including decreased cell population across males and females. Embryonic forebrain transcriptomics revealed sex-specific alterations. Autism relevant developmental pathways were downregulated in male forebrain, driven by genes including *Reln* and *Lama1*. Altered genes in female forebrain were enriched for autism-risk genes including *Grin2b* and *Dync1h1*. Following these transcriptomic differences, postnatal neurobehavioral trajectories were sex specific. Male offspring uniquely showed reduced motor learning, increased stereotyped behaviors, altered reversal learning, and reduced forebrain neuronal number. Female offspring displayed opposite behavioral changes as males and few changes in forebrain structure.

Conclusions:

The provision of *Igf1* specifically from placenta is critical for offspring forebrain development. This temporary early deficit has persistent sex-specific neurobehavioral effects. These outcomes have relevance for autism risk and highlight mechanisms that could facilitate intervention development for adverse outcomes after early loss of placental hormone support in perinatal adversity.

Introduction:

Preterm birth increases the risk for neurodevelopmental disorders (NDDs), including autism spectrum disorder (ASD) (1-3). Improved survival rates among preterm infants have coincided with an increased prevalence of these conditions (1, 4, 5) but mechanisms are not understood. Both preterm birth and NDDs are associated with other perinatal adversities involving placental dysfunction and insufficiency (6-8). Preterm birth causes early loss of placental support, including hormones critical for neurodevelopment (9, 10). This includes insulin-like growth factor 1 (IGF1), an essential hormone that influences both placental function and neurodevelopment (11-14). Levels of IGF1 and associated proteins at birth predict growth and neurodevelopment in placental insufficiency and preterm infants as well as birth weight in term babies (15-18).

How IGF1 from placenta specifically influences the brain has been minimally studied. IGF1 is primarily produced by endothelial cells in the placental fetal region (19, 20). Within the placenta, IGF1 promotes hormone and nutrient transport necessary for fetal development via IGF1 receptor (IGF1R) signaling (11). Within the brain, IGF1 regulates and promotes growth, with high forebrain expression of IGF1R (13, 21, 22). IGF1 promotes forebrain cell cycle progression and differentiation across cell types (13, 22). Total *Igf1* knockout in mice reduces adult brain weight and parvalbumin-containing neurons in the hippocampus and striatum (22, 23). On the flipside, total *Igf1* overexpression in mice increases embryonic and juvenile brain weight and cell number in forebrain subregions including the cerebral cortex and caudate-putamen (24). Additionally, placental *Igf1* overexpression increases embryonic striatal growth and alters striatal neurons and striatal-dependent, NDD-relevant behaviors postnatally (13).

Morphological changes to the forebrain and its subregions are associated with NDDs, particularly the striatum which has been shown to be sensitive to changes in IGF1 (13, 22, 23). Changes in striatal morphology and function are linked to ASD and ADHD (25-27), including restricted, repetitive behaviors, motor regulation, and procedural and reversal learning (25, 28). Additionally, individuals with ASD have decreased IGF1 in serum and CSF (29-31). Together these studies provide insight into early IGF1 insufficiency from placenta as a possible mechanism of risk for NDDs from preterm birth and adversity involving placental insufficiency. No published work has evaluated this mechanism of placental IGF1 insufficiency for neurodevelopmental risk (9, 13).

In this study we aimed to determine whether placental *Igf1* insufficiency can drive translationally relevant outcomes, emphasizing the importance of the striatum. Placental *Igf1* insufficiency was created using placental-targeted CRISPR manipulation (32) Significant changes in striatal development were identified in males and relevant to ASD risk. These findings are critical as they identify possible therapeutic targets for impacts of perinatal neurodevelopmental risks including prematurity and placental insufficiency.

Materials and Methods:

<u>Animal Husbandry and Care</u>

CD-1 mice purchased from Charles River or bred in house were used for CRISPR manipulation experiments. Tpbpαr/Adaf-AdaP-cre mice (33) were provided by Dr. Yang Xia's laboratory at Texas A&M Health Science Center and bred to create the placenta-cre line with Jax *Igf1* flox mice (34) as homozygotes. Mouse handling and husbandry were performed as approved by the University of Iowa IACUC (protocol 3121284). Mice were housed in a 12-hour light cycle with food and water ad libitum.

Placental-Targeted CRISPR Manipulation

Placental-targeted CRISPR manipulation was performed as previously described (32). IGF-I CRISPR/Cas9 KO Plasmid (m) and Control CRISPR/Cas9 plasmids (Santa Cruz Biotechnology) were diluted to 0.073 µg/µl. Litters collected at embryonic timepoints had individual placentas injected with either IGF1 knockout or control plasmid, but litters used for postnatal assessments were treated with only one type of plasmid as previously described (13).

Sex Genotyping

Sex was determined for embryonic samples via PCR assessing *Jarid* or *Rmb31* genotype. Tpbpαr/Adaf-AdaP-cre/*Igf1* flox (i.e. placenta-cre) animals were genotyped using *Cre* and *Igf1* flox PCR primers (**Supplemental Table 1**).

Quantitative Polymerase Chain Reaction

Placentas from CRISPR manipulated litters were collected as previously described (13). Placentas from placenta-cre litters were cut in half laterally. One half had the decidua removed while the other retained the decidua to parse expression changes due to maternal influence. RNA was isolated using the Trizol method and concentrations were normalized prior to cDNA synthesis. PowerSYBR Master Mix was used for qPCR on the ViiA 7 Real-Time PCR System (Thermo Scientific). Gene expression was normalized to the housekeeping gene *18s.* See supplemental table 1 for primer sequences. The ddct method was used to generate normalized fold change from same-sex controls.

Placental Histology

5µm placental sections were H&E stained then visualized on the Axio Imager M.2 microscope (Zeiss). The area of placenta subregions was measured using StereoInvestigator (Microbrightfield) from two sections and averaged.

Embryonic and Adult Brain Analysis

Embryonic day (E) 14 and E18 heads were fixed, cryoprotected, and serially sectioned at 25 µm. Adult brains were collected approximately 2 weeks after behavior completion via transcardial perfusion with saline followed by 4% PFA, cryoprotected, serially sectioned at 50 µm, blocked with 10% horse serum, and immunostained in 10% horse serum/phosphate buffered saline with antibodies for NeuN (Cell Signaling, rabbit monoclonal, catalog #12943) (1:300) or GFAP (Invitrogen, rabbit polyclonal, catalog #10019) (1:500) followed by the appropriate secondary (Thermo Fischer Scientific, goat anti-rabbit, Alexa-Fluor 594, catalog #A-11012) (1:500) and mounted with Vectashield with DAPI (Vector Labs). Every 20th embryonic and every 10th adult section of each brain was visualized on an Axio Imager M.2 microscope (Zeiss) and StereoInvestigator (Microbrightfield) was used to quantify region volumes and unbiased stereology of cell populations using consistent counting frames and randomly placed grids in the “optical fractionator” workflow.

Forebrain RNA Sequencing

E18 forebrains were microdissected, stored in RNAlater, and processed for RNA using the RNAeasy Mini Kit (Qiagen). RNA concentrations were quantified using Qubit and quality was evaluated by Bioanalyzer. Only high-quality RNA (RIN >8) was used. RNA samples were sequenced on Illumina NovaSeq (Novogene). Illumina adapters were removed using TrimGalore (v 0.6.6) and aligned to the mm10 reference transcriptome and then quantified using Salmon (v 1.10.1). Mapping efficiency was sufficient across samples (**Supplemental Table 2**). Using R Studio, differentially expressed genes (DEGs) were identified using DESeq2 (v 1.46.0) (35). All results were generated separately by sex and with litter as covariate. Using the svaseq function from the sva package (v 3.54.0) one surrogate variable was used for both males and females to control for unwanted variation (36). Significance was defined by a false discovery rate (FDR) of <0.05. DEGS were compared to the SFARI database list of autism-relevant genes from the 7/8/25 release list. Gene set enrichment analyses (GSEA) were performed for the DEGs identified from DESeq2 via the GSEA program (v4.4.0) to identify different enriched biological processes between treatment groups. Significance was defined as FDR<0.05 and a trend as FDR<0.1.

Maternal Behavior

Dams with manipulated litters were monitored as previously reported (13). On postnatal day (P) 0, P3, P8, and P14 dams were recorded starting in the light cycle for 24, 3, 2, and 1 hours respectively. Dams were analyzed in four-minute increments and scored by a blinded experimenter to assess maternal time on and off the nest.

Behavioral Testing

Juvenile (P26-28) or early adult (P56+) mice were behaviorally tested as previously described (13). All testing was done after habituation in home cages for a minimum of 30 minutes during the light cycle with task order as follows, least to most stressful.

Open Field Testing (OFT)

Mice were individually placed inside a plexiglass OFT apparatus, recorded for 30 minutes, then analyzed using ANYmaze (Stoelting) to assess distance and center time in the first five minutes and throughout.

Rotarod

Rotarod testing was performed for two consecutive days, 5 trials each day. Mice were placed on the apparatus (Ugo Basile) and accelerated from 4 to 80 rpm over 240 seconds. Holding onto the rod for two full revolutions or falling concluded the trial; duration recorded. Learning coefficients were calculated as the difference of the average trial length of the last 2 trials (4 and 5 of day two) and average trial length of the first 2 trials (1 and 2 from day one). Weighted learning coefficients were then generated as the learning coefficient divided by the average of the first 2 trials.

Y-Maze

Mice were placed in the same starting position in a Y-shaped apparatus (Stoelting), and arm entries were recorded for 5 minutes. Spontaneous alternation was calculated as proportion of alternating entry triplets to total arm entry triplets.

Elevated Plus Maze (EPM)

Mice were placed into the center of the apparatus (Stoelting) and recorded for 5 minutes for assessment of open arm time using ANYmaze (Stoelting).

Water T Maze

A T-shaped maze was placed in a tub filled with water mixed with nontoxic white paint to obfuscate a platform inside one arm beneath the water's surface. Water T maze consists of two phases: habit and reversal. For the habit phase, mice were trained to find the hidden platform for 10 trials per day until training criterion was met: 5 consecutive trials with no incorrect arm entry (i.e. error). Training continued for 2 more days after criterion. For the reversal phase, the platform was moved to the opposite arm and trials proceeded only until criterion was met. Errors were recorded until both criteria were met. Habit and reversal learning performance were

assessed by number of errors and trials before criterion, correcting trial number for lead-in trials on each day.

Stereotypy

Mice were video recorded for 20 minutes in a rectangular plexiglass chamber. The number of stereotyped behaviors were scored by a blinded observer in 1-minute increments every 5 minutes.

Autism-Relevant Behavior Composite Score

An autism-relevant behavior composite score to compare degree of difference in behavior versus same-sex controls was generated for each mouse as previously described (10, 13). Each behavioral result was z-scored within each sex and the absolute values of z-scores were averaged. Included results were: OFT total distance, OFT total center time, Y-maze score, EPM open arm time, water T maze habit errors, water T maze reversal errors, and total stereotyped behaviors.

Statistical Analysis

All statistical analysis was performed separately by sex for offspring outcomes. The ROUT test was used to remove outliers. The linear mixed effects model (lmer) with litter as a random effect in R was used for embryonic and placental analyses (13). Postnatal and maternal measures were analyzed (Graphpad Prism) using Welch's t-test or Mann-Whitney test (if F variance score failed) (13). Placenta-cre analyses were run with either Welch's t test or two-way ANOVA with post-hoc comparisons that did not include litter as a covariate due to few pairings.

Results:

Successful creation of placental Igf1 insufficiency model

Multiple methods were considered to reduce placental *Igf1,* including two placental-specific Cre transgenic lines: Cyp19-cre is expressed within a subset of trophoblasts and Tpbpαr/Adaf-AdaP-cre is expressed in most trophoblasts (33, 37). Since Tpbpαr/Adaf-AdaP-cre has more extensive expression, this line was bred with an *Igf1* flox line (**Supplemental Figure 1A**) (34). Placental *Igf1* expression was not reduced in total placenta; only after isolation of the fetal zones to eliminate the unaffected source of *Igf1* from maternal decidua cells was a decrease in expression detected (**Supplemental Figure 1B-D**). Body and placental mass were reduced regardless of cre, suggesting undesirable impacts of the floxed line alone (**Supplemental Figure 1E-H**). No change was detected in embryonic forebrain development (**Supplemental Figure 1I-L**). This model was not pursued due to these multiple limitations.

Placental-targeted CRISPR manipulation was used to knockout *Igf1* on E12 to assess whether insufficiency would influence placental, embryonic, and postnatal neurobehavioral outcomes (**Figure 1A**). The *Igf1* knockout (IGF1-KO) CRISPR plasmid containing three guide RNAs (**Figure 1B**) successfully reduced placental *Igf1* expression approximately 32% across both sexes (**Figure 1C**). As previously reported, female placental *Igf1* was lower at baseline than males (**Supplemental Figure 2A**) (13). Due to these findings, the placental-targeted CRISPR manipulation was used as the more effective method to create placental *Igf1* insufficiency.

There were few changes to placental structure and function from reduced placental *Igf1,* allowing this model to reproduce more precisely an insufficient supply of IGF1 to the fetus. E14 Igf1-KO male placentas demonstrated minor compensations in IGF signaling expression that may promote placental IGF1 signaling, while E18 males as well as E14 and E18 females did not (**Supplemental Figure 2B,C**). Angiogenic factors were unchanged, amino acid transporter expression was minimally altered, and placental subregions were unchanged (**Supplemental Figure 2D-F**). Despite this, Igf1-KO females, but not males, had decreased placental and body mass at several timepoints, with body mass recovered by the juvenile timepoint (**Supplemental Figure 2G**) supporting the insufficient supply of IGF1 for only prenatal growth.

Placental Igf1 insufficiency impairs embryonic forebrain development

Forebrain morphology was assessed at E14 and E18 to evaluate the impact of placental Igf1-KO on early neurodevelopment. No changes in E14 ganglionic eminence volume or total cell population or cortical volume were identified, but an early decrease in forebrain volume was seen only in females (**Supplemental Figure 3A-E**). By E18, striatal volume and total cell population were reduced in both males and females (**Figure 2A-C**). E18 females had decreased forebrain white matter volume, fiber tracts which support striatal-cortical connectivity (**Figure 2D**). There was also decreased forebrain volume (**Figure 2E**) and trend decreased cortical volume across sexes at E18 (**Supplemental Figure 3F**), brain phenotypes relevant to preterm infant outcomes.

Sex-specific ASD-relevant transcriptional changes in embryonic forebrains

E18 forebrain transcriptomic analysis identified changes relevant to ASD-risk (**Figure 3A-C and Supplemental Figure 4A,B**). The DEGs identified in Igf1-KO males and females compared to same-sex controls did not overlap, demonstrating clear sex-specific changes in E18 forebrain (**Supplemental Table 3 and 4**). Some key DEGs inform these different effects. In males, upregulation was found for *Cacna2d4,* a gene influencing neuromotor development, as the most significantly changed DEG (38). In females, results showed the most significant DEG change was downregulation of *Huwe1*, a gene for a ubiquitin ligase that influences neuronal proliferation and differentiation (39).

GSEA analysis to identify changes in biological processes revealed none in females. In contrast, Igf1-KO males had multiple significant or trending downregulated key biological processes (**Figure 3D and Supplemental Table 5**). As expected, these included insulin-like growth factor receptor signaling. Igf1-KO male forebrain had unexpected downregulation of hormone biosynthesis, specifically C21 steroid hormones. These include pregnenolone and testosterone, which may influence the trajectory of sexually dimorphic neurodevelopmental processes (40, 41). Additionally, there was a downregulation of external encapsulating structure organization (i.e., extracellular matrix) and endoderm development and formation, all involving differential expression of multiple laminin genes (*Lama1, Lama5, and Lamc1*) and *Reln*. Not only do these genes play critical roles in cell biology of the developing brain, but they are also ASD risk genes (42). DEGs from Igf1-KO male and female forebrains were assessed for enrichment for SFARI ASD-risk genes. While ASD-risk genes were not enriched in male forebrain DEGs (p=0.1578 and odds ratio=2.4), three of these were established ASD-risk genes (**Figure 3E**). The DEGs identified in Igf1-KO female forebrains were enriched for ASD-risk genes, identifying six established ASD-risk genes (p=0.0048** and odds ratio=4.5) (**Figure 3E**). Most of the ASD-risk genes found in females are implicated in synapse processes (43-48). Both male and female DEGs that overlapped with SFARI risk genes were in the top two gene score groups indicating a high confidence association with ASD-risk (**Figure 3E**). These findings demonstrate that reduction of IGF1 from placenta sex-specifically affects the brain even at embryonic stages in ways overlapping with ASD-risk.

ASD-relevant behavioral deficits in juvenile Igf1-KO mice

We next examined how temporary placental *Igf1* insufficiency could influence neurobehavior persistently into postnatal development. First, maternal care across four postnatal timepoints was found to be unchanged by the placental CRISPR manipulations (**Supplemental Figure 5A-F**), making further outcomes more likely to be due to altered placental *Igf1* directly.

To understand impacts on juveniles P26 to P28, motor activity, exploration, and motor learning were assessed. The first five minutes of locomotor activity was increased in Igf1-KO females and trend increased in males (**Figure 4A,B**). Igf1-KO males had increased center time within this same period (**Figure 4C**). These findings demonstrate an acute behavioral response to novelty, potentially due to increased stress susceptibility as the mice adjust to the test chamber (49, 50). This was supported by no distance or center time differences across all 30 min of open field testing (**Figure 4D,E**). Rotarod testing revealed Igf1-KO males improved less with motor learning, while females showed no deficit (**Figure 4G,H**). These neurodevelopmental impacts were present even weeks after the initial placental *Igf1* insufficiency.

Adult Igf1-KO males and females demonstrate opposite changes to ASD-relevant behavior

Behavior was assessed in early adulthood to determine lasting impacts relevant to striatal function and ASD. Adult Igf1-KO showed more changes in striatal-dependent

outcomes—habit/reversal learning and stereotyped behaviors—but less in domains such as working memory and anxiety-relevant behavior (**Supplemental Figure 6A-F**). While no differences in water T maze trials to habit learning criterion were identified in males or females across groups, Igf1-KO females had increased errors in habit learning and increased trials to reach reversal learning criterion (**Figure 5A-C and Supplemental Figure 6G**). Interestingly, Igf1-KO males performed better than controls on water T maze reversal learning (**Figure 5C,D**). Stereotyped behavior analysis further identified opposite changes in Igf1-KO males and females, as males had increased stereotyped behaviors while females had a decrease (**Figure 5E,F**). The differences on these tasks suggest disrupted striatal development and/or function (25). To compare behaviors across domains, ASD-relevant behavior composite scores were generated from adult behavioral tests as previously described (10, 13) demonstrating distinct behavioral changes in Igf1-KO males and females (**Figure 5G-J**). These results persist months after placental *Igf1* insufficiency, demonstrating a potential mechanism for ASD-relevant behavior after perinatal adversity.

Placental Igf1 insufficiency results in sex-specific persistent changes to the forebrain

The neurobiological underpinnings of behavioral changes were investigated by assessing adult forebrain structure and cell composition. As previously found after placental *Igf1* overexpression, striatal and cortical volumes that were affected embryonically no longer showed group differences (**Figure 6A,B and Supplemental Figure 7A,B**) (13). However, adult Igf1-KO females unexpectedly showed a trend increase in forebrain white matter volume (**Figure 6C**) along with normalization of striatal cell and neuron number. (**Figure 6D-F**). By contrast, Igf1-KO males had normal forebrain white matter and decreased striatal neurons (**Figure 6C-F**). A similar decrease of male prefrontal cortex neurons demonstrated that this effect affected multiple forebrain regions (**Supplemental Figure 7C-E**). No difference was found in the striatal astrocytes, a cell subtype that primarily arises postnatally (**Figure 6G-I**) (51). These sex-specific brain outcomes occurred in the context of sex differences in embryonic forebrain transcriptomic response to *Igf1* insufficiency which may represent the earliest stage in the pathway to these effects. Regardless, decreased placental *Igf1* had a strong influence on the forebrain, even postnatally, relevant to NDD risk after preterm birth.

Discussion:

This study identified that forebrain developmental and behavioral outcomes in mice relevant to NDDs can be driven by placental *Igf1* loss. Placental-targeted CRISPR manipulation allowed us to create a hypomorphic *Igf1* knockout that modeled an insufficiency of hormone support similar to preterm birth, placental insufficiency, and other perinatal risks for NDDs (9, 10, 15-18, 32). Placental Igf1-KO mice had reduced embryonic forebrain growth, including specifically reduced striatal volume and cell density across sexes. However, sex-specific forebrain transcriptional changes suggested distinct developmental pathways in males and females alongside these overall structural effects. Following this, juvenile and adult behavior changes were distinct across sexes. The interaction between sex and early placental *Igf1*

support of brain development was further emphasized by sex-specific changes in adult brain morphology and structure. Overall, placental *Igf1* insufficiency resulted in persistent effects on neurodevelopment and behavior that implicate this insufficiency as a possible mechanism of perinatal adversity contributing to NDD and ASD risk (**Figure 7**).

Decreased embryonic forebrain and striatal volumes accompanied by decreased striatal total cell population in E18 Igf1-KO males and females demonstrated a clear initial effect on forebrain growth and development after placental *Igf1* insufficiency. This recapitulates human phenotypes that link low IGF1 levels with decreased brain volume after preterm birth (18). Despite E18 striatal morphology not showing sex-specificity, transcriptional changes in the E18 forebrain did not overlap in Igf1-KO males and females. Females demonstrated a significant enrichment of ASD-risk genes in embryonic forebrain DEGs which demonstrates one mechanism through which placental *Igf1* insufficiency may increase NDD-risk. Additionally, E18 Igf1-KO female forebrains demonstrated a significant downregulation of *Huwe1*, a gene highly associated with intellectual disability, which is well-established as a major regulator of cell-cycle progression (39, 52). This downregulation emphasizes placental IGF1's role in cell cycle regulation in neurodevelopment as similarly shown with a placental *Igf1* overexpression model (13). Additionally, most of the ASD-risk genes identified in Igf1-KO female forebrains are involved in synapse formation and function, key processes implicated in ASD, highlighting another possible mechanism in which placental *Igf1* insufficiency may increase NDD-risk (43-48). While the forebrain and striatum structurally normalized by adulthood, striatal-dependent behaviors were altered in females but in ways distinct from males, suggesting that the early distinct transcriptomics may have had lasting impacts. Interestingly, Igf1-KO females uniquely had increased adult forebrain white matter volume, the opposite of the embryonic deficit but still associated at the group level with learning disruptions. In a total *Igf1* knockout mouse model, an initial decrease in embryonic myelin-specific proteins was found to reverse in adulthood (53), suggesting that the greater forebrain white matter seen in Igf1-KO females may have occurred through secondary impacts after *Igf1* insufficiency. Additionally, a model of placental allopregnanolone insufficiency also demonstrated sex-specific changes to myelination (10, 54).

In contrast, the influence of placental *Igf1* insufficiency on males resulted in early deficits in forebrain development which persisted. Early effects included a downregulation in the forebrain of IGF1R signaling, essential laminin genes, and hormone synthesis. While these results cannot be correlated with behavior, a decrease in perinatal hormone synthesis, particularly C21 steroids including testosterone and many others (55), may influence NDD risk for males from this mechanism. Additionally, Igf1-KO males had a reduction in forebrain neurons which may contribute to downregulation of steroid hormone synthesis as neurons are primarily responsible for local hormone synthesis within the brain (55, 56). Interestingly, the behavioral changes displayed by juvenile and adult males mostly resulted in behavioral phenotypes comparable to control females. This is somewhat in line with the general finding that female placentas express less *Igf1*, and this lower placenta *Igf1* may be one way that neurobehavioral outcomes are similarly shaped.

This study builds upon previous research demonstrating placental hormone insufficiency as critical mechanisms for NDD risk. Similar to this study, placental allopregnanolone

insufficiency in mice sex-specifically alters neurodevelopment and behavior relevant to ASD (9, 10, 54). Furthermore, a knockout of the placenta-specific transcript of *Igf2* resulted in anxiety-like behavior and altered synaptic receptor expression in the hippocampus (57). Lastly, our study builds upon a previous work that inhibited IGF1R activity in the early postnatal brain to model preterm birth in mice at a timepoint relevant to late *in utero* human brain development (58). This study identified similar changes to neurodevelopment, including decreased neuron populations in the prefrontal cortex and increased stereotyped behaviors (58). Our study expands upon this by isolating the role of placental *Igf1* on neurodevelopment.

While this study is highly informative, all brain regions and processes were not investigated, making it possible that other alterations are relevant to placental *Igf1* insufficiency. Additionally, the timing of placental *Igf1* effects on neurodevelopment will invariably be different in mice than humans with perinatal adversity, as mouse brains are less developed than humans at birth. Despite these limitations, this study effectively demonstrates a clear role of placental *Igf1* in neurodevelopment that is informative for preterm birth and NDDs.

As preterm birth is associated with NDDs that are highly prevalent, it is crucial to understand how early loss of placental hormonal support impacts neurodevelopment. This study highlights a crucial role of placental *Igf1* in neurodevelopment and its strong association with ASD-risk. The findings of this and similar studies emphasize the potential of early detection as well as intervention for placental hormone production anomalies in conditions such as preterm birth, intrauterine growth restriction, and placental insufficiency. This research will contribute to intervention development in infants at risk for NDDs and may aid in the creation of *in utero* treatments, as the placenta is an accessible target during prenatal development.

Acknowledgements:

The authors would like to acknowledge the following funding sources: National Institute of Mental Health grant R01MH122435 (HES), National Institute of General Medical Sciences grants T32GM008629 and T32GM145441 (AJC), National Center for Advancing Translation Science R25TR004393 (AG), Graduate College, University of Iowa (AJC), and Pappajohn Biomedical Institute, University of Iowa (FMF and BWQH). The authors would like to thank Dr. Yang Xia's laboratory at Texas A&M Health Science Center for providing us with their Tpbpα/Adaf-AdaP-cre mouse line. The authors would like to thank Dr. Val Sheffield and Dr. Calvin Carter's labs at the University of Iowa for the use of their surgery room and equipment. We would also like to thank the Genomics Core at the University of Iowa. Figure 1A, figure 1B, figure 3A, figure 4A&F, figure 5A&E, and figure 7 (graphical conclusion) were created using BioRender.com Carver, A. (2026) https://BioRender.com/98ah0o5, https://BioRender.com/560kv8r, https://BioRender.com/3l1ahqd, https://BioRender.com/sgrxpq8, https://BioRender.com/lie9v89, and https://BioRender.com/71lhn49.

Author Contributions

Conceptualization, A.J.C. and H.E.S.; data curation, A.J.C and B.W.Q.H.; formal analysis, A.J.C., B.W.Q.H, and H.E.S.; funding acquisition A.J.C., F.M.F., B.W.Q.H, A.G., and H.E.S.; investigation A.J.C., F.M.F., R.J.T., B.W.Q.H., A.G., and R.T.F.; methodology, A.J.C., R.J.T., B.W.Q.H, and H.E.S.; project administration, A.J.C., R.J.T., and H.E.S.; resources, H.E.S.; supervision, A.J.C. and H.E.S.; validation, A.J.C. and R.J.T.; visualization, A.J.C., F.M.F., B.W.Q.H., A.G., and R.T.F.; writing—original draft, A.J.C., F.M.F., R.J.T., A.G., and R.T.F.; writing—review & editing, A.J.C., F.M.F., R.J.T., B.W.Q.H., and H.E.S.

Disclosures: The authors have nothing to disclose.

Data Availability: Upon publication, the transcriptomic data will be deposited in the Gene Expression Omnibus database. All other data will be available upon request.

Figures:

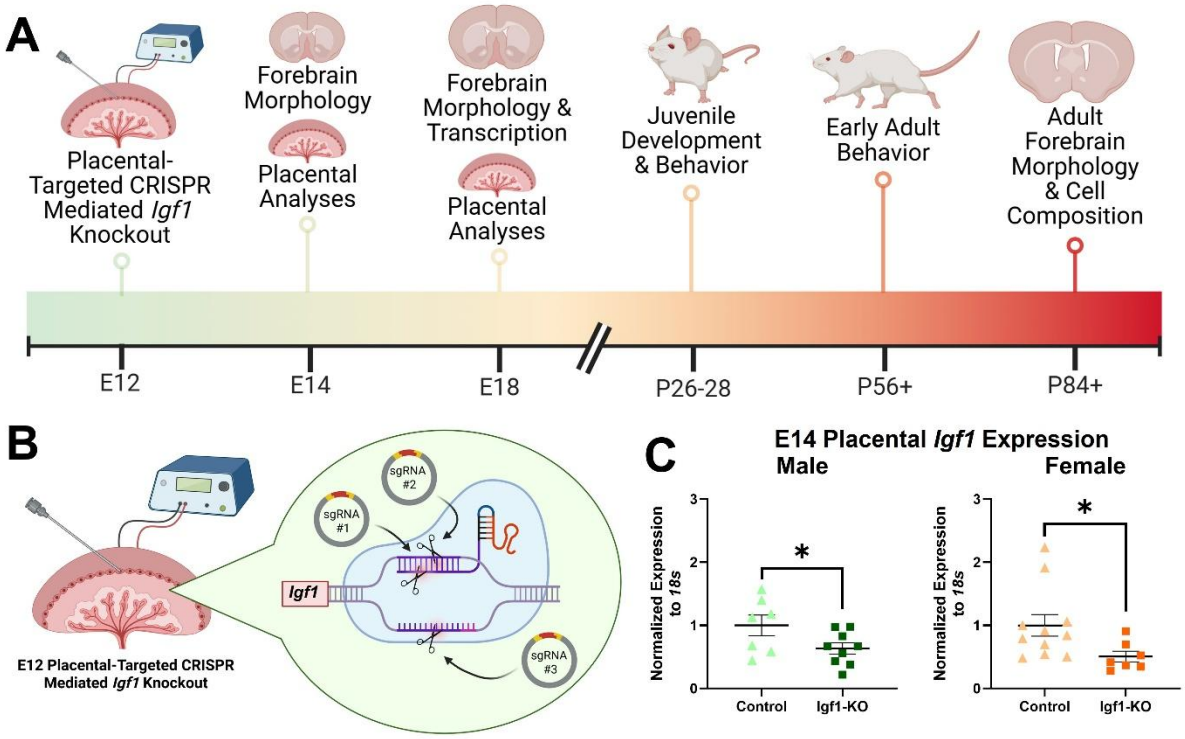

Figure 1. Successful creation of placental *Igf1* insufficiency model. (A) Schematic of project timeline. **(B)** Schematic of E12 placental-targeted CRISPR mediated *Igf1* knockout. **(C)** Placental *Igf1* expression normalized to *18s* in E14 Igf1-KO males and females (n=7-11 per group). Both graphs show mean and SEM. *p < 0.05 by linear mixed effects model with litter as random effect.

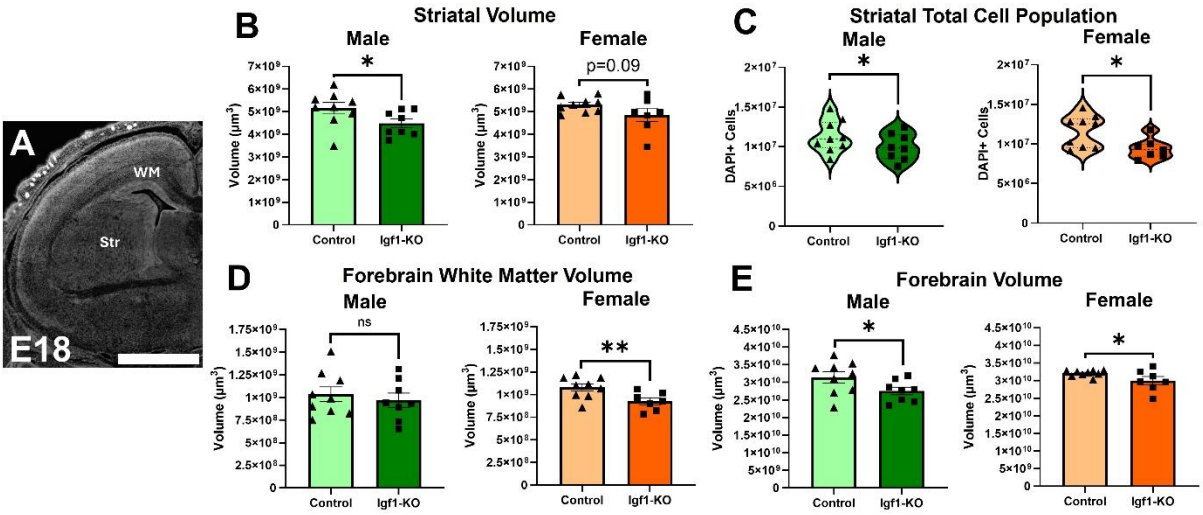

Figure 2. Placental *Igf1* insufficiency impairs embryonic forebrain development. (A) Representative image of a coronal hemisection of E18 forebrain stained with DAPI, striatum (Str) and forebrain white matter (WM) labeled. **(B)** E18 male and female striatal volume (n=7-9 per group). **(C)** E18 male and female striatal total cell (DAPI) population (n=7-9 per group). **(D)** E18 male and female forebrain white matter volume (n=7-9 per group). **(E)** E18 male and female forebrain volume (n=7-9 per group). Scale bar displays 1mm in panels A. All graphs show mean and SEM except for panel C which display median and quartiles. ns=nonsignificant, trending p<0.1, and *p < 0.05 by linear mixed effects model with litter as random effect.

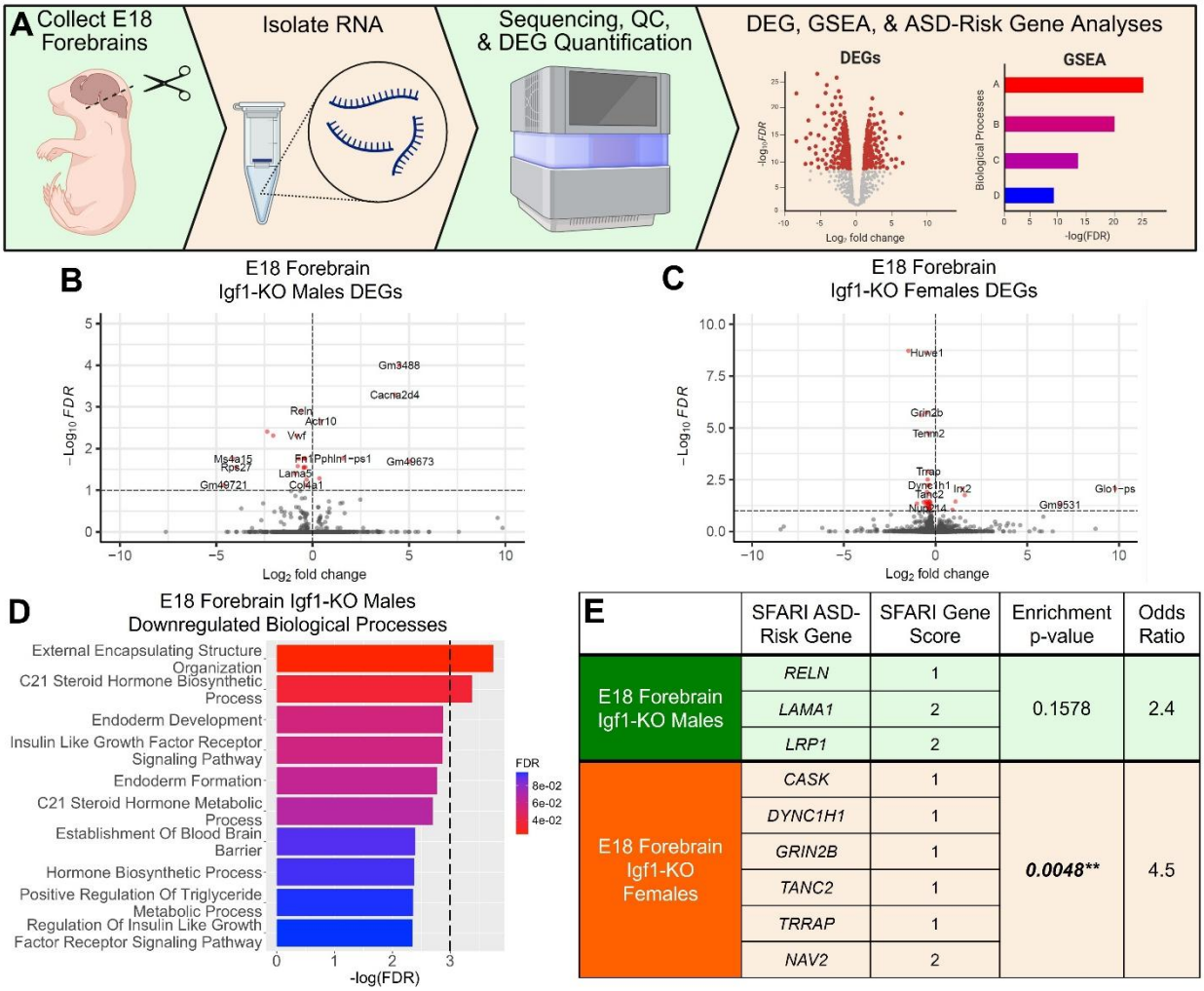

	SFARI ASD-Risk Gene	SFARI Gene Score	Enrichment p-value	Odds Ratio
E18 Forebrain Igf1-KO Males	*RELN*	1	0.1578	2.4
	LAMA1	2		
	LRP1	2		
E18 Forebrain Igf1-KO Females	*CASK*	1	***0.0048***	4.5
	DYNC1H1	1		
	GRIN2B	1		
	TANC2	1		
	TRRAP	1		
	NAV2	2		

Figure 3. Sex-specific ASD-relevant transcriptional changes in embryonic forebrains. (A) Schematic of RNAsequencing workflow. Volcano plots showing DEGs from E18 Igf1-KO **(B)** male and **(C)** female forebrains compared to same-sex controls (n=6 per group). Scaling adjusted for readability, full volcano plots in supplement. **(D)** Key downregulated biological pathways in E18 Igf1-KO male forebrains identified using GSEA. Dashed line represents FDR = 0.05. Bars above this line (FDR < 0.05) represent significant change while bar graphs below this line (FDR < 0.1 but above 0.05) show trending change. **(E)** A table highlighting DEGs from E18

Igf1-KO male and female forebrains that are listed in the SFARI-ASD risk gene dataset (n=6 per group); significance defined as p<0.05.

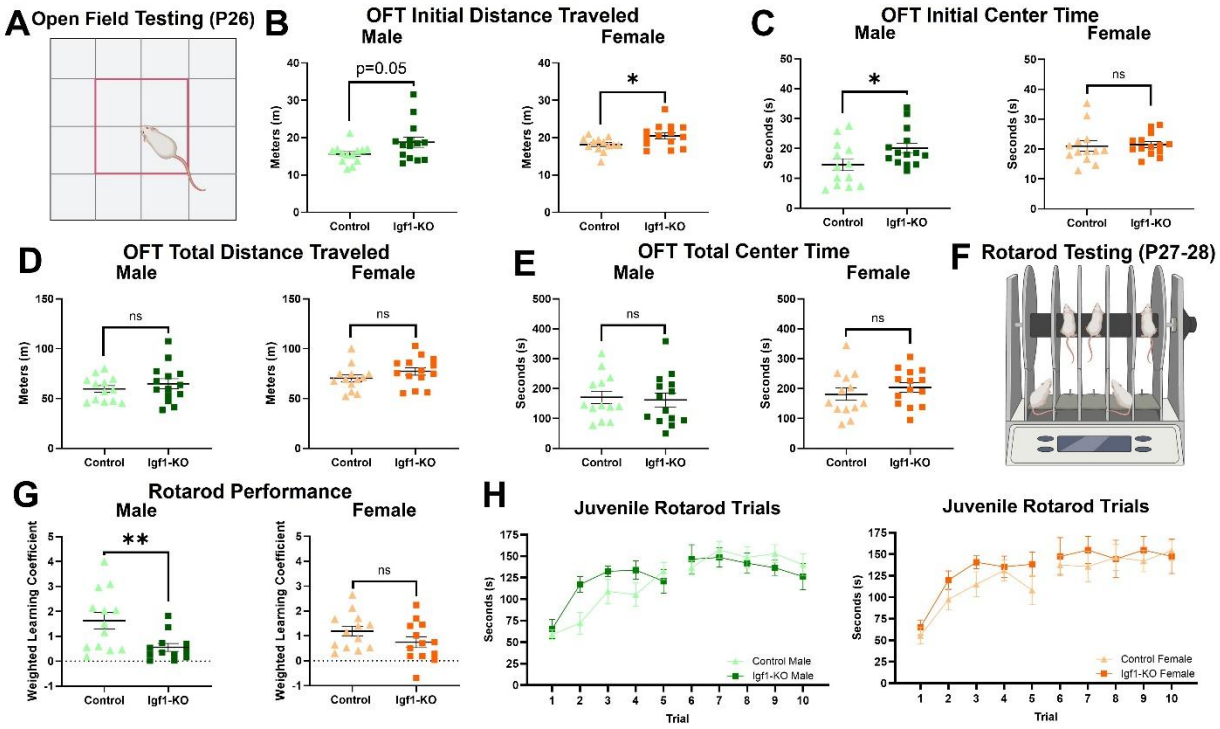

Figure 4. ASD-relevant behavioral deficits in juvenile Igf1-KO mice. (A) Representative graphic of open field testing (OFT). **(B)** Juvenile male and female distance traveled in the initial period (first 5 minutes) of OFT (n=13-14 per group). **(C)** Juvenile male and female center time in the initial period of OFT (n=13-14 per group). **(D)** Juvenile male and female distance traveled for the total time (30 minutes) of OFT (n=13-14 per group). **(E)** Juvenile male and female center time for the total time of OFT (n=13-14 per group). **(F)** Representative graphic of rotarod testing. **(G)** Juvenile male and female rotarod performance displayed as weighted learning coefficient (n=12-13 per group). **(H)** Graph of group means for each rotarod trial (n=12-13 per group). All graphs show mean and SEM. ns=nonsignificant, trending p<0.1, *p < 0.05, and **p<0.01 by Welch's t-test.

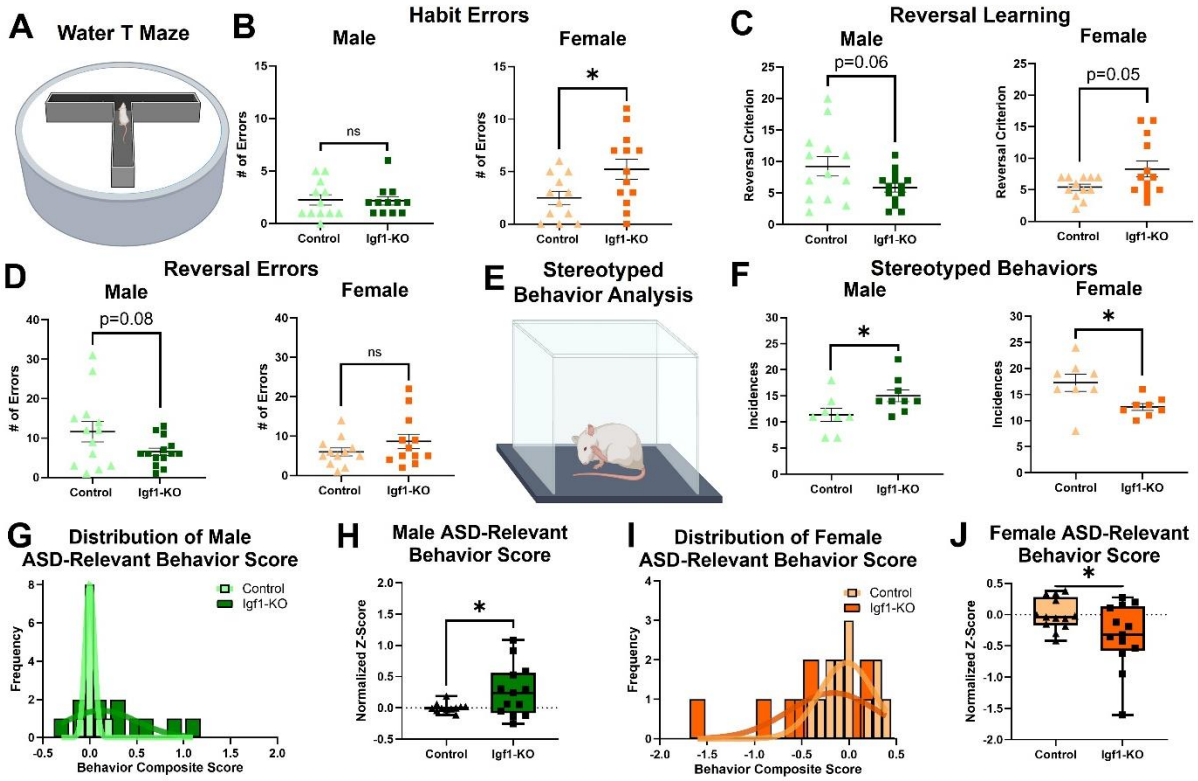

Figure 5. Adult Igf1-KO males and females demonstrate opposite changes to ASD-relevant behavior. (A) Representative graphic of the water T maze. **(B)** Number of errors made by adult male and females during water T maze habit training (n=12-13 per group). **(C)** Reversal learning in water T maze in adult male and females scored as reversal criterion (n=12-14 per group). **(D)** Number of errors made by adult male and females during water T maze reversal testing (n=12-14 per group). **(E)** Representative graphic of stereotyped behavior testing. **(F)** Incidences of adult male and female stereotyped behaviors (n=8-9 per group). **(G)** Distribution of adult male ASD-relevant behavior composite scores (n=11-13 per group). **(H)** Adult male ASD-relevant behavior composite score displayed as normalized z-score (n=11-13 per group). **(I)** Distribution of adult female ASD-relevant behavior composite scores (n=13 per group). **(J)** Adult female ASD-relevant behavior composite score displayed as normalized z-score (n=13 per group). All graphs show mean and SEM except panels H and J which show median and quartiles. ns=nonsignificant, trending $p<0.1$, and $*p < 0.05$ by Welch's t-test.

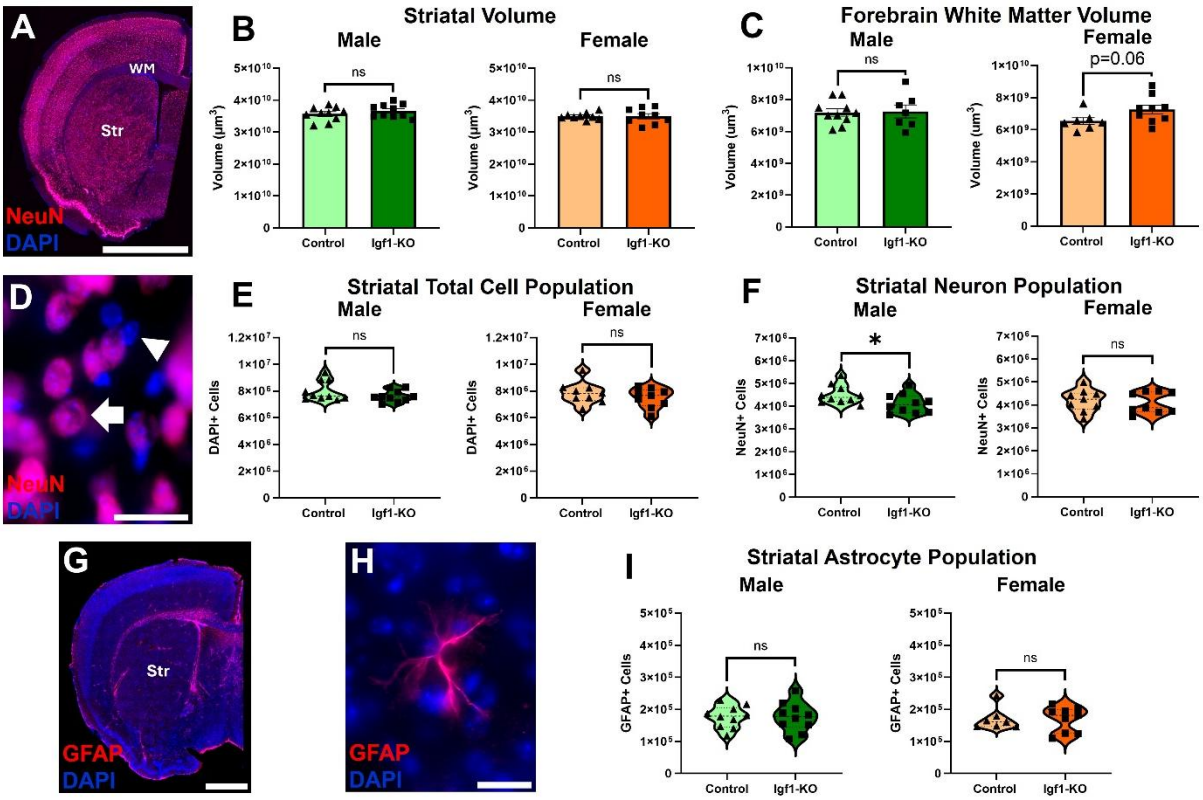

Figure 6. Placental *Igf1* insufficiency results in sex-specific persistent changes to the forebrain. (A) Representative image of a coronal hemisection of adult forebrain stained with DAPI (blue) and NeuN (red). Striatum (Str) and forebrain white matter (WM) labeled. **(B)** Adult male and female striatal volume (n=9-10 per group). **(C)** Adult male and female forebrain white matter volume (n=7-10 per group). **(D)** Representative image of DAPI (blue) and NeuN (red) staining in the adult striatum, arrow points to NeuN+ and DAPI+ cell and the arrowhead points to a DAPI+ cell. **(E)** Adult male and female striatal total cell (DAPI) population (n=9-10 per group). **(F)** Adult male and female striatal neuron (NeuN) population (n=9-10 per group). **(G)** Representative image of a coronal hemisection of adult forebrain stained with DAPI (blue) and GFAP (red). Striatum (Str) labeled. **(H)** Representative image of GFAP (red) staining in the adult striatum. **(I)** Adult male and female striatal astrocyte (GFAP) population (n=7-10 per group). Scale bars display 2mm in panel A, 25µm in panel D, 1mm in panel G, and 20µm in panel H. Graphs in panels B and C show mean and SEM. Graphs in panels E, F, and I show median and quartiles. ns=nonsignificant, trending $p<0.1$, and $*p < 0.05$ by Welch's t-test.

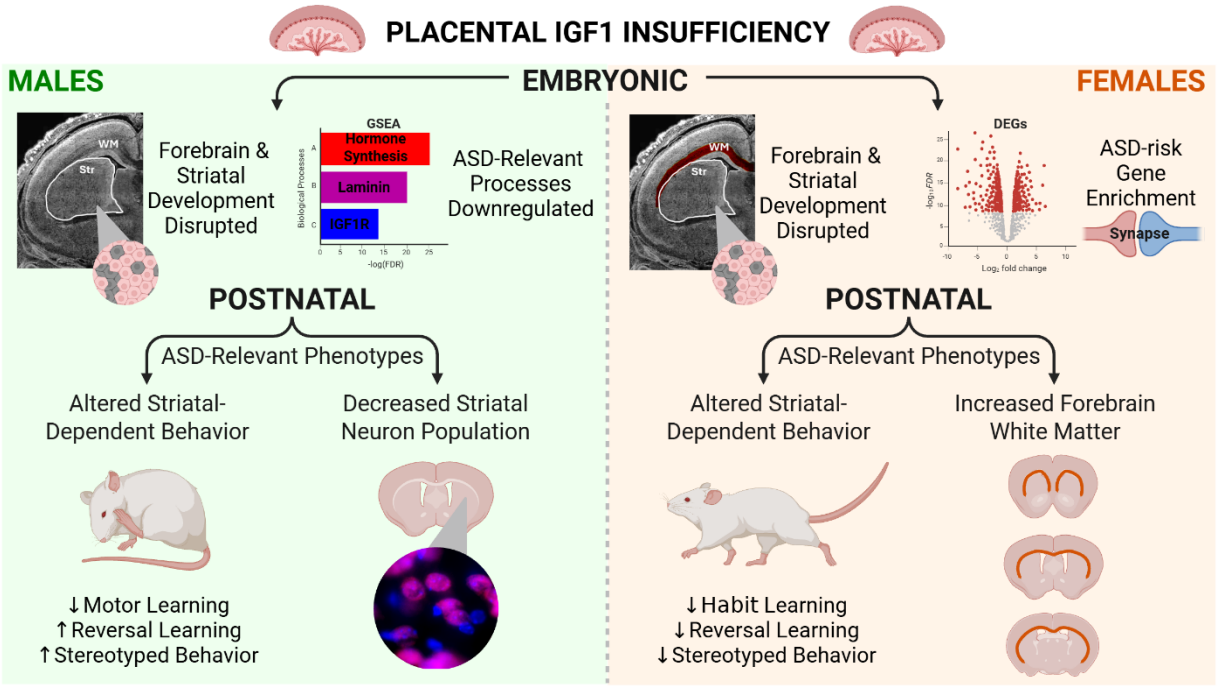

Figure 7. Graphical summary.

References:

1. Hee Chung E, Chou J, Brown KA (2020): Neurodevelopmental outcomes of preterm infants: a recent literature review. *Transl Pediatr*. 9:S3–S8.
2. Crump C, Sundquist J, Sundquist K (2021): Preterm or Early Term Birth and Risk of Autism. *Pediatrics*. 148.
3. Fraiman YS, Guyol G, Acevedo-Garcia D, Beck AF, Burris H, Coker TR, et al. (2023): A Narrative Review of the Association between Prematurity and Attention-Deficit/Hyperactivity Disorder and Accompanying Inequities across the Life-Course. *Children (Basel)*. 10.
4. Maenner MJ, Warren Z, Williams AR, Amoakohene E, Bakian AV, Bilder DA, et al. (2023): Prevalence and Characteristics of Autism Spectrum Disorder Among Children Aged 8 Years - Autism and Developmental Disabilities Monitoring Network, 11 Sites, United States, 2020. *MMWR Surveill Summ*. 72:1–14.
5. Reuben C, Elgaddal N (2024): Attention-Deficit/Hyperactivity Disorder in Children Ages 5-17 Years: United States, 2020-2022. *NCHS Data Brief*.1–9.
6. Morgan TK (2016): Role of the Placenta in Preterm Birth: A Review. *Am J Perinatol*. 33:258–266.
7. Rosenfeld CS (2021): The placenta-brain-axis. *Journal of Neuroscience Research*. 99:271–283.
8. Baschat AA (2011): Neurodevelopment following fetal growth restriction and its relationship with antepartum parameters of placental dysfunction. *Ultrasound Obstet Gynecol*. 37:501–514.
9. Bakalar D, O'Reilly JJ, Lacaille H, Salzbank J, Ellegood J, Lerch JP, et al. (2022): Lack of placental neurosteroid alters cortical development and female somatosensory function. *Front Endocrinol (Lausanne)*. 13:972033.
10. Vacher CM, Lacaille H, O'Reilly JJ, Salzbank J, Bakalar D, Sebaoui S, et al. (2021): Placental endocrine function shapes cerebellar development and social behavior. *Nat Neurosci*. 24:1392–1401.
11. Sferruzzi-Perri AN, Sandovici I, Constancia M, Fowden AL (2017): Placental phenotype and the insulin-like growth factors: resource allocation to fetal growth. *The Journal of Physiology*. 595:5057–5093.
12. Steinman G (2020): The putative etiology and prevention of autism. *Prog Mol Biol Transl Sci*. 173:1–34.
13. Carver AJ, Fairbairn FM, Taylor RJ, Boggarapu S, Kamau NR, Gajmer A, et al. (2025): Placental Igf1 overexpression sex-specifically impacts mouse placenta structure, altering offspring striatal development and behavior. *Exp Neurol*. 394:115453.
14. Carver AJ, Dunnwald M, Stevens HE (2025): A head start: The relationship of placental factors to craniofacial and brain development. *Dev Dyn*.
15. Leviton A, Allred EN, Fichorova RN, VanderVeen DK, O'Shea TM, Kuban K, et al. (2019): Early Postnatal IGF-1 and IGFBP-1 Blood Levels in Extremely Preterm Infants: Relationships with Indicators of Placental Insufficiency and with Systemic Inflammation. *Am J Perinatol*. 36:1442–1452.

16. Paulsen ME, Marka N, Nagel EM, Gonzalez Villamizar JD, Nathan BM, Ramel SE (2024): An exploratory study of clinical factors associated with IGF-1 and IGFBP-3 in preterm infants. *Pediatr Res*. 96:402–408.
17. Lagiou P, Samoli E, Hsieh CC, Lagiou A, Xu B, Yu GP, et al. (2014): Maternal and cord blood hormones in relation to birth size. *Eur J Epidemiol*. 29:343–351.
18. Hansen-Pupp I, Hovel H, Hellstrom A, Hellstrom-Westas L, Lofqvist C, Larsson EM, et al. (2011): Postnatal decrease in circulating insulin-like growth factor-I and low brain volumes in very preterm infants. *J Clin Endocrinol Metab*. 96:1129–1135.
19. Dalcik H, Yardimoglu M, Vural B, Dalcik C, Filiz S, Gonca S, et al. (2001): Expression of insulin-like growth factor in the placenta of intrauterine growth-retarded human fetuses. *Acta Histochem*. 103:195–207.
20. Hiden U, Glitzner E, Hartmann M, Desoye G (2009): Insulin and the IGF system in the human placenta of normal and diabetic pregnancies. *J Anat*. 215:60–68.
21. Dyer AH, Vahdatpour C, Sanfeliu A, Tropea D (2016): The role of Insulin-Like Growth Factor 1 (IGF-1) in brain development, maturation and neuroplasticity. *Neuroscience*. 325:89–99.
22. Wrigley S, Arafa D, Tropea D (2017): Insulin-Like Growth Factor 1: At the Crossroads of Brain Development and Aging. *Front Cell Neurosci*. 11:14.
23. Beck KD, Powell-Braxton L, Widmer HR, Valverde J, Hefti F (1995): Igf1 gene disruption results in reduced brain size, CNS hypomyelination, and loss of hippocampal granule and striatal parvalbumin-containing neurons. *Neuron*. 14:717–730.
24. Popken GJ, Hodge RD, Ye P, Zhang J, Ng W, O'Kusky JR, et al. (2004): In vivo effects of insulin-like growth factor-I (IGF-I) on prenatal and early postnatal development of the central nervous system. *Eur J Neurosci*. 19:2056–2068.
25. Evans MM, Kim J, Abel T, Nickl-Jockschat T, Stevens HE (2024): Developmental Disruptions of the Dorsal Striatum in Autism Spectrum Disorder. *Biol Psychiatry*. 95:102–111.
26. O'Dwyer L, Tanner C, van Dongen EV, Greven CU, Bralten J, Zwiers MP, et al. (2016): Decreased Left Caudate Volume Is Associated with Increased Severity of Autistic-Like Symptoms in a Cohort of ADHD Patients and Their Unaffected Siblings. *PLoS One*. 11:e0165620.
27. Soghomonian JJ (2023): The cortico-striatal circuitry in autism-spectrum disorders: a balancing act. *Front Cell Neurosci*. 17:1329095.
28. Grill F, Guitart-Masip M, Johansson J, Stiernman L, Axelsson J, Nyberg L, et al. (2024): Dopamine release in human associative striatum during reversal learning. *Nat Commun*. 15:59.
29. Abedini M, Mashayekhi F, Salehi Z (2022): Analysis of Insulin-like growth factor-1 serum levels and promoter (rs12579108) polymorphism in the children with autism spectrum disorders. *J Clin Neurosci*. 99:289–293.
30. Li Z, Xiao GY, He CY, Liu X, Fan X, Zhao Y, et al. (2022): Serum levels of insulin-like growth factor-1 and insulin-like growth factor binding protein-3 in children with autism spectrum disorder. *Zhongguo Dang Dai Er Ke Za Zhi*. 24:186–191.

31. Riikonen R, Makkonen I, Vanhala R, Turpeinen U, Kuikka J, Kokki H (2006): Cerebrospinal fluid insulin-like growth factors IGF-1 and IGF-2 in infantile autism. *Dev Med Child Neurol*. 48:751–755.
32. Carver AJ, Taylor RJ, Stevens HE (2023): Mouse In Vivo Placental Targeted CRISPR Manipulation. *J Vis Exp*.
33. Zhou CC, Chang J, Mi T, Abbasi S, Gu D, Huang L, et al. (2012): Targeted expression of Cre recombinase provokes placental-specific DNA recombination in transgenic mice. *PLoS One*. 7:e29236.
34. Liu JL, Grinberg A, Westphal H, Sauer B, Accili D, Karas M, et al. (1998): Insulin-like growth factor-I affects perinatal lethality and postnatal development in a gene dosage-dependent manner: manipulation using the Cre/loxP system in transgenic mice. *Mol Endocrinol*. 12:1452–1462.
35. Love MI, Huber W, Anders S (2014): Moderated estimation of fold change and dispersion for RNA-seq data with DESeq2. *Genome Biol*. 15:550.
36. Leek JT, Johnson WE, Parker HS, Jaffe AE, Storey JD (2012): The sva package for removing batch effects and other unwanted variation in high-throughput experiments. *Bioinformatics*. 28:882–883.
37. Wenzel PL, Leone G (2007): Expression of Cre recombinase in early diploid trophoblast cells of the mouse placenta. *Genesis*. 45:129–134.
38. Klomp A, Omichi R, Iwasa Y, Smith RJ, Usachev YM, Russo AF, et al. (2022): The voltage-gated Ca2+ channel subunit alpha2delta-4 regulates locomotor behavior and sensorimotor gating in mice. *PLoS One*. 17:e0263197.
39. Zhao X, Heng JI, Guardavaccaro D, Jiang R, Pagano M, Guillemot F, et al. (2008): The HECT-domain ubiquitin ligase Huwe1 controls neural differentiation and proliferation by destabilizing the N-Myc oncoprotein. *Nat Cell Biol*. 10:643–653.
40. Vacher CM, Tsompanidis A, Firestein MR, Penn AA (2025): Neuroactive steroid exposure impacts neurodevelopment: Comparison of human and rodent placental contribution. *J Neuroendocrinol*. 37:e13489.
41. Jansakova K, Hill M, Celarova D, Celusakova H, Repiska G, Bicikova M, et al. (2020): Alteration of the steroidogenesis in boys with autism spectrum disorders. *Transl Psychiatry*. 10:340.
42. Long KR, Huttner WB (2021): The Role of the Extracellular Matrix in Neural Progenitor Cell Proliferation and Cortical Folding During Human Neocortex Development. *Front Cell Neurosci*. 15:804649.
43. Becker M, Mastropasqua F, Reising JP, Maier S, Ho ML, Rabkina I, et al. (2020): Presynaptic dysfunction in CASK-related neurodevelopmental disorders. *Transl Psychiatry*. 10:312.
44. Eschbach J, Sinniger J, Bouitbir J, Fergani A, Schlagowski AI, Zoll J, et al. (2013): Dynein mutations associated with hereditary motor neuropathies impair mitochondrial morphology and function with age. *Neurobiol Dis*. 58:220–230.
45. Elmasri M, Lotti JS, Aziz W, Steele OG, Karachaliou E, Sakimura K, et al. (2022): Synaptic Dysfunction by Mutations in GRIN2B: Influence of Triheteromeric NMDA Receptors on Gain-of-Function and Loss-of-Function Mutant Classification. *Brain Sci*. 12.

46. Garrett L, Da Silva-Buttkus P, Rathkolb B, Gerlini R, Becker L, Sanz-Moreno A, et al. (2022): Post-synaptic scaffold protein TANC2 in psychiatric and somatic disease risk. *Dis Model Mech*. 15.
47. Muley PD, McNeill EM, Marzinke MA, Knobel KM, Barr MM, Clagett-Dame M (2008): The atRA-responsive gene neuron navigator 2 functions in neurite outgrowth and axonal elongation. *Dev Neurobiol*. 68:1441–1453.
48. Guang S, Pang N, Deng X, Yang L, He F, Wu L, et al. (2018): Synaptopathology Involved in Autism Spectrum Disorder. *Front Cell Neurosci*. 12:470.
49. Shoji H, Takao K, Hattori S, Miyakawa T (2016): Age-related changes in behavior in C57BL/6J mice from young adulthood to middle age. *Mol Brain*. 9:11.
50. Reiber M, Koska I, Pace C, Schonhoff K, von Schumann L, Palme R, et al. (2022): Development of behavioral patterns in young C57BL/6J mice: a home cage-based study. *Sci Rep*. 12:2550.
51. Chaboub LS, Deneen B (2013): Astrocyte form and function in the developing central nervous system. *Semin Pediatr Neurol*. 20:230–235.
52. Giles AC, Grill B (2020): Roles of the HUWE1 ubiquitin ligase in nervous system development, function and disease. *Neural Dev*. 15:6.
53. Ye P, Li L, Richards RG, DiAugustine RP, D'Ercole AJ (2002): Myelination is altered in insulin-like growth factor-I null mutant mice. *J Neurosci*. 22:6041–6051.
54. Salzbank J, Lacaille H, Gaby J, O'Reilly JJ, Kissner M, Vacher CM, et al. (2025): Microglia alter sex-specific cerebellar myelination following placental hormone loss. *Nat Commun*. 16:9846.
55. Balan I, Boero G, Chery SL, McFarland MH, Lopez AG, Morrow AL (2024): Neuroactive Steroids, Toll-like Receptors, and Neuroimmune Regulation: Insights into Their Impact on Neuropsychiatric Disorders. *Life (Basel)*. 14.
56. Day M, Belal M, Surmeier WC, Melendez A, Wokosin D, Tkatch T, et al. (2024): GABAergic regulation of striatal spiny projection neurons depends upon their activity state. *PLoS Biol*. 22:e3002483.
57. Mikaelsson MA, Constancia M, Dent CL, Wilkinson LS, Humby T (2013): Placental programming of anxiety in adulthood revealed by Igf2-null models. *Nat Commun*. 4:2311.
58. Potenzieri A, Uccella S, Preiti D, Pisoni M, Rosati S, Lavarello C, et al. (2024): Early IGF-1 receptor inhibition in mice mimics preterm human brain disorders and reveals a therapeutic target. *Sci Adv*. 10:eadk8123.